



1 **Interaction between East Asian summer monsoon and west winds as**
2 **shown by tree-ring records**

3

4 Shengchun Xiao^{1*}, Xiaomei Peng¹, Quanyan Tian¹, Aijun Ding², Jiali Xie¹, Jingrong
5 Su^{1 3}

6

7 ¹ Key Laboratory of Ecological Safety and Sustainable Development in Arid Lands,
8 Northwest Institute of Eco-Environment and Resources, Chinese Academy of
9 Sciences, Lanzhou, Gansu, China 730000.

10 ² College of Resources and Environment, Gansu Agricultural University, Lanzhou,
11 Gansu, China 730070.

12 ³ University of Chinese Academy of Sciences, Beijing, China 100049.

13 * Corresponding author (xiaosc@lzb.ac.cn).

14 Address: 320 West Donggang Road, Lanzhou City, Gansu Province, China.

15 Zip Code: 730000.

16



17 **Abstract:**

18

19 Against the background of changes in global atmospheric circulation, local changes in
20 the East Asian summer monsoon (EASM) and the mid-latitude westerly winds will
21 inevitably affect the climate and ecology of the arid zone of Northwest China. Hence,
22 it is important to study these changes. We chose to observe these changes in the Alxa
23 Plateau using dendrochronological methods. We assembled ring-width records from
24 Qinghai spruce trees growing in the mountain regions surrounding the Alxa Plateau:
25 the Helan Mountains, Changling Mountain, and Dongdashan Mountain. We analyzed
26 these records for changes on interannual and interdecadal scales. Our results show that
27 radial growth was indeed affected by changes in the monsoons and westerlies. The
28 heterogeneity of precipitation and climatic wet-dry changes in different regions is
29 primarily influenced by the interactions between atmospheric circulation systems, each
30 with its own dominant controlling factors. In the case of the Helan Mountains, both of
31 these major atmospheric circulation systems play a significant role in shaping climate
32 changes. Changling Mountain in the southern part of the Alxa Plateau are mainly
33 influenced by the EASM. Dongdashan Mountain is mainly influenced by the westerlies.
34 Understanding these local conditions will help us predict climate changes in Northwest
35 China.

36

37 **Key words:** Alxa Plateau, dendroclimatology, westerly winds, EASM, interaction
38 between winds and monsoon

39

40



41 **1. Introduction**

42 **1.1 Importance of climate studies in northwestern China**

43 The alpine zone of Qinghai-Tibet, the arid zone of the northwestern interior, and the
44 humid zone of the east constitute the three main areas of China's natural
45 geomorphology (Chen et al., 2019b). The Northwest China inland dry zone is located
46 in the hinterland of the Eurasian continent and is among the driest regions in the world.
47 It exhibits typical continental climatic characteristics. This region is mainly influenced
48 by westerly winds and the EASM. The interaction of these two factors results in high
49 precipitation variability and hence frequent droughts. This would be the case even
50 before global climate change began affecting the area; it is even more the case in current
51 years. This inland dry zone is very much an ecologically fragile area (Chen et al., 2019a;
52 Chen et al., 2019b; Zhang et al., 2023).

53 The semi-arid and arid regions of northern China are characterized by large areas
54 of sand and desert. They are the second largest source of dust in the world after the
55 Sahara. Their contribution to global climate change is large. So far inland, the influence
56 of the EASM is often weak (Zhang et al., 2021; Liu et al., 2022). It is opposed by the
57 westerly winds that flow from the North Atlantic climate zone toward the East Asian
58 monsoon climate zone (Qu et al., 2004). The interaction between the westerly winds
59 and the EASM governs precipitation, water vapor transport, and thus the climate of
60 northwestern China (Feng et al., 2004; Wang et al., 2005; Li et al., 2008; Ma et al.,
61 2011).

62 It is important to understand the history of this interaction if we are to estimate how
63 global climate change will affect it. Global atmospheric circulation is likely to change
64 as is the EASM. Climate change will not only affect the regional climate and regional
65 water resources (Ding et al., 2023); it will affect East Asia (dust storms) and even the
66 rest of the globe. Hence the study of climate in this region is of great practical and
67 theoretical significance (Chen et al., 2019a; Chen et al., 2019b).

68 The westerly winds and the EASM meet at the northern boundary of the Asian
69 summer monsoon (Huang et al., 2023). In northern China, this boundary runs from west
70 to east, along the eastern section of the Qilian Mountains, the southern foothills of the



71 Helan Mountains, the Daqing Mountains, and the western section of the Daxinganling
72 Mountains. This is not a static boundary. It fluctuates within a range of 200–700 km
73 (Chen et al., 2018). It is important to understand the history of these fluctuations (Huang
74 et al., 2023).

75 This can be done using climate records such as lacustrine, eolian, and
76 dendrochronological (Sun et al., 2003; Liu et al., 2005; Li, 2009; Chen et al., 2010; Li
77 et al., 2016; Chen et al., 2019b; Qin et al., 2023). Our research team specializes in
78 dendrochronology, which is one of the best tools for studying paleoclimatic changes,
79 due to its precise dating, high resolution, good continuity and high replication (Zhang
80 et al., 2003; Shao et al., 2010; Yang et al., 2014; Liu et al., 2016).

81

82 1.2 Previous work

83 The climate history of the Baotou area, at the northern edge of the EASM, has been
84 studied at interannual and interdecadal scales for the past 260 years, based on June–
85 August precipitation reconstruction from tree-ring samples from the western Yinshan
86 Mountains (Liu et al., 2001; Liu et al., 2003). Using tree-rings and historical records,
87 Kang and Yang (2015) reconstructed the annual precipitation history of the East Asian
88 monsoon northern fringe zone for the last 530 years. They analyzed spatial variability
89 and possible driving mechanisms using the 400-mm isohyet.

90 Several May–July precipitation sequences have been reconstructed using ring-
91 width and latewood-width data from Chinese pine (*Pinus tabulaeformis*) growing in
92 the Helan Mountains (Ma et al., 2003; Liu et al., 2004; Chen et al., 2016). Studies of
93 tree-ring carbon and oxygen isotopes from Chinese pine samples have shown that $\delta^{18}\text{O}$
94 values increase with summer precipitation, while $\delta^{13}\text{C}$ values decrease (Zhang et al.,
95 2005a; Liu et al., 2008). Westerly winds have also been shown to affect precipitation in
96 the Helan Mountains (Chen et al., 2010).

97 Principal component analysis of tree-ring chronologies constructed from data
98 collected at several sites in Gansu suggests that trees at these sites were more influenced
99 by EASM than by west winds (Chen et al., 2013). These researchers also found that the
100 EASM weakened in 1970s, but recovered in the early 1990s. Tree-ring data allowed the



101 reconstruction of 330 years of PDSI values for the Mount Hasi region (at the northern
102 boundary of the summer monsoon zone) (Kang et al., 2012). This study confirmed that
103 radial growth of Chinese pine has declined over the past three decades, due to the
104 weakening of the EASM. Dendrochronological reconstruction of precipitation in the
105 Mount Changling region (again using Chinese pine) suggested that precipitation in that
106 region mainly depends on the EASM (Chen et al. 2012). Other researchers have
107 assembled tree-ring chronologies from pines growing in the Mount Qilian region and
108 the northern mountains of the Hexi Corridor. Here again precipitation is associated with
109 the EASM. These chronologies have allowed scholars to compile precipitation,
110 temperature, and drought records for the last thousand years (Gou et al., 2015a; Gou et
111 al., 2015b; Zhang et al., 2017).

112 Most modern researchers studying climate change in the region are mostly carried
113 out on single sample sites (Wang et al., 2004; Liu et al., 2005; Chen et al., 2010; Chen
114 et al., 2016; Li et al., 2016; Liu et al., 2016; Chen et al., 2018). There is a dearth of
115 multi-site, regional, **large-scale studies** on the interaction of the westerlies and the
116 EASM. **Our group** compiled and analyzed tree-ring chronologies from Qinghai spruce
117 (*Picea crassifolia*) growing in the Helan, Changling, and Dongdashan mountain regions
118 that surround the Alxa Plateau, the climate response characteristics of spruce radial
119 growth in three regions was then analyzed. Combining the relevant Westerly and East
120 Asia monsoon circulation indices, the driving mechanism of the regional climate
121 change by with the interaction and synergistic roles of two atmospheric circulation
122 systems in the Alxa Plateau was explored. The results will lay a theoretical foundation
123 for the climatic evolution of the region and the desertification control.

124

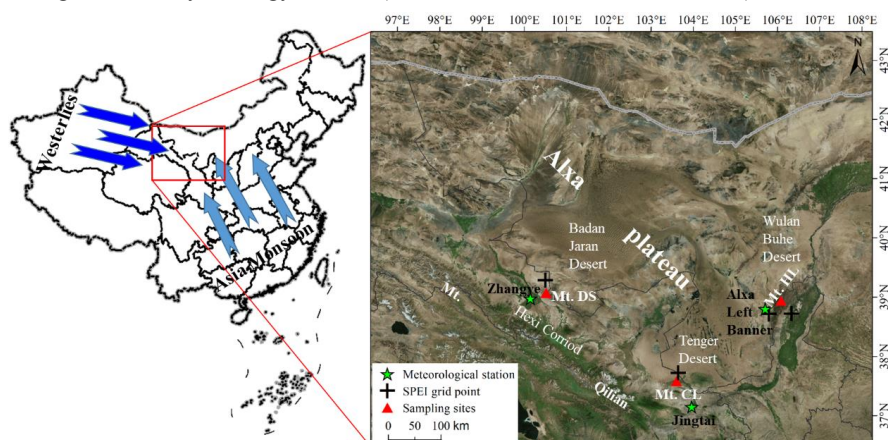
125 **2. Material and methods**

126 **2.1 Study area**

127 The Alxa Plateau is located in the western part of the Inner Mongolia Autonomous
128 Region and is surrounded by mountains (Fig.1). It consists primarily of three deserts:
129 Tengger, Ulan Buh, and Badan Jaran. It lies south of the Gobi desert. It is the main
130 source of the fierce sandstorms and dust storms that blow toward eastern China and the



131 Pacific. It has been much affected by climate change; sand- and dust storms have
132 increased, much to the detriment of lands to the east. The Chinese government is doing
133 what it can to establish an environmental defense line there. It is currently the Northern
134 Sand Prevention Belt of the National Two Ecological Barrier and Three Belts
135 Ecological Security Strategy Pattern (Xiao et al., 2017; Xiao et al., 2019).



136
137 Figure 1. Location of tree-ring sampling sites and meteorological stations (the right
138 panel is from Mapworld)

139 There are several mountain ranges surrounding the Alxa Desert, such as the Helan
140 Mountains in the east, the northern mountains of the Hexi Corridor, and the outliers of
141 the Altai Mountains in the north. These mountains not only block the eastward and
142 southward expansion of the desert (driven by high pressure regions from Mongolia);
143 they are also the source of mountain rivers and streams that water the oases on the
144 plateau.

145 The Alxa Plateau is located in the eastern margin of the inland arid region of Central
146 Asia. It is affected not only by the mid-latitude westerly circulation, but also by the
147 Asian monsoon and the plateau monsoon. It is in the zone where the mid-latitude
148 westerly circulation and the Asian monsoon interact (Xiao et al., 2017; Chen et al.,
149 2019b). As a result, there is large interannual variability of vegetation cover in the
150 region (Ou and Qian, 2006; Tang et al., 2006; Li et al., 2013).

151 The Helan Mountains ($38^{\circ}27' \sim 39^{\circ}30'N$, $105^{\circ}20' \sim 106^{\circ}41'E$) (sampling site
152 henceforth abbreviated as HL), are located at the eastern edge of the Tengger Desert.



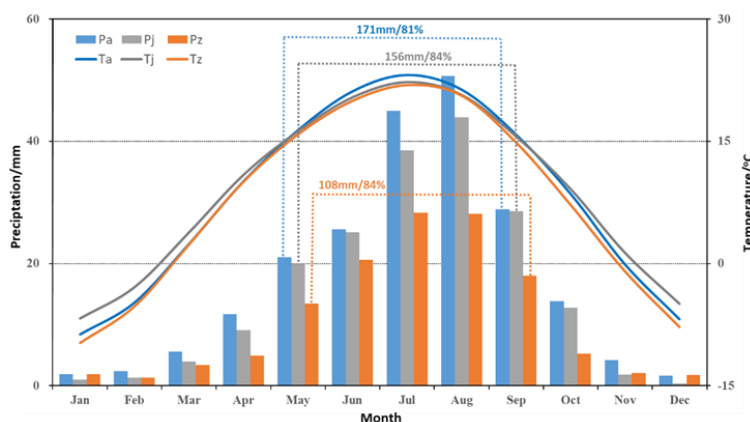
153 They stretch more than 200 kilometers from north to south; the main peak is ~3,556 m.
154 The mountain forests are dominated by Qinghai spruce and Chinese pine, juniper,
155 mountain aspen, and elm.

156 Mount Changling (37°12'~37°17', 102°45'~103°48'E) (sampling site henceforth
157 abbreviated as CL) is an independent mountain protruding northward from the
158 remnants of the eastern Qilian Mountains, It is located at the southern edge of the
159 Tengger Desert; its elevations range from 2100 to 2900 m. The dominant tree species
160 are Qinghai spruce and Chinese pine.

161 Mount Dongdashan (39°00'~39°04'N, 100°45'~100°51'E) (sampling site
162 henceforth abbreviated as DS) is located at the southwestern edge of the Badan Jaran
163 Desert and the middle part of Mount Qilian. It is one of the northern mountains along
164 the Hexi Corridor; that range consists of mountains that vary from 2200 to 2637 m in
165 elevation. Forests are dominated by Qinghai spruce and Qilian juniper.

166 The temperatures of the coldest months recorded at meteorological stations in the
167 Alxa Left Banner (a division of the Alxa League region), Jingtai (a county in Gansu),
168 and Zhangye (a city in Gansu) all occurred in January, ranging from -9.8°C to -6.8°C.
169 The hottest months at those stations were in July (21.9°C to 23.1°C). These
170 meteorological stations are the closest stations to our three sampling sites.

171 Precipitation measured at those stations varied widely. The multi-year average of
172 total precipitation from May to September was 171 mm at Alxa Left Banner station,
173 156 mm at Jingtai station, and 108 mm at Zhangye station. This accounted for more
174 than 80% of the annual precipitation (Fig.2).



175

176 Figure 2. Climatic diagram of study area. Pa/Ta are the monthly total precipitation and
177 monthly mean temperature at the Alxa Left Banner meteorological station (1953–2016);
178 Pj/Tj are the precipitation and temperature figures for the Jingtai meteorological station
179 (1957–2017); Pz/Tz are the precipitation and temperature figures for the Zhangye
180 meteorological station (1957–2017). The dashed box and appended data indicate the
181 total growing season precipitation in the study area and the proportion of total annual
182 precipitation.

183

184 2.2 Sample collection, processing and data analysis method

185 2.2.1 Sample collection, processing and dendrochronology construction

186 Researchers used standard methods of tree-ring sample collection. One core was drilled
187 from each tree in the sample site. We collected 209 cores in total, from five sampling
188 sites at HL, 48 cores from one sampling site at CL, and 81 cores from two sampling
189 sites at DS. Relevant information re the sampling sites is summarized in Table 1.

190 Chronologies were constructed using standard dendrochronological methods. We
191 calculated the highly significant correlations ($P < 0.001$) between the chronologies of
192 different points at the HL and DS mountains; a weighting method was used to finally
193 synthesize a chronology for each mountain.

194

195 2.2.2 Climate data, atmospheric circulation indices and the related Analyzing 196 methods for chronological correlation



197 Climate data for the study areas HL, CL, and DS were collected from the nearest
198 meteorological stations in Alxa Left Banner, Jingtai and Zhangye, respectively
199 (<http://data.cma.cn>).

200 We used **SPEI** to represent the local drought and wetness conditions. SPEI data
201 (grid-point resolution $0.5^{\circ} \times 0.5^{\circ}$) was obtained from the grid-point datasets of the
202 National Center for Environmental Predictions-National Center for Atmospheric
203 Research (NCEP-NCAR). Time scales ranged from 1 month to 15 months. The mean
204 values of data from two grid-points closest to the HL sampling site ($38.75^{\circ}\text{N}, 105.75^{\circ}\text{E}$
205 and $38.75^{\circ}\text{N}, 106.25^{\circ}\text{E}$; period 1953–2015) were chosen for subsequent analysis. Grid-
206 point data from one site closest to our CL sampling site ($37.75^{\circ}\text{N}, 103.75^{\circ}\text{E}$; period 1951–
207 2015) was used for later analysis. Grid-point data from one site closest to our DS
208 sampling site ($39.25^{\circ}\text{N}, 100.75^{\circ}\text{E}$; period 1951–2015) was also used. As SPEI datasets
209 are multi-scale, we preprocessed the data to identify and select 11-month scaled SPEI
210 datasets for subsequent analysis.

211 We took into account the so-called lagging effect (the influence of fall and winter
212 climate factors on the radial growth of trees shows up later in the year) and chose to use
213 temperature, precipitation, and SPEI data from September of the previous year to
214 September of the current year (abbreviated as P9–P12 and C1–C9), as collected at each
215 meteorological station, for our climate response analysis.

216 **The East Asian Summer Monsoon Index (EASMI)** represents the activity strength
217 of the EASM. Larger EASMI values indicate a stronger summer monsoon, smaller ones
218 a weaker monsoon. In this study, the EASMI (mean values for June–August in the
219 period 1950–2017) defined by Li and Zeng (2005) was used to study the impact of the
220 EASM on climate change in the study area.

221 We used the **Westerly Circulation Index (WCI annual mean)** to represent the
222 strength of the mid-latitude westerlies. The larger the WCI value, the stronger the
223 Eurasian latitudinal circulation; the smaller the value, the weaker the Eurasian
224 latitudinal circulation. WCI data (period 1951–2015) were derived from the Eurasian
225 Latitudinal Circulation Index published by the National Climate Center of the China
226 Meteorological Administration (<https://cmdp.ncc-cma.net/cn/index.htm>).



227 Interannual and interdecadal (sliding moving average of 11a) chrono-climatic/
228 cyclonic index correlation and partial correlation analyses were performed using SPSS
229 19.0. Based on the characteristics of tree-ring series, the sequences were classified into
230 three groups of low, average and high ring widths using $\text{mean} \pm 1\delta$ (SD) as the
231 classification criterion (with $\text{mean} \pm 2\delta$ as the extreme year). Correlation statistical tests
232 were performed with the corresponding annual circulation indices; similar treatments
233 and analyses were performed for the two major circulation indices.

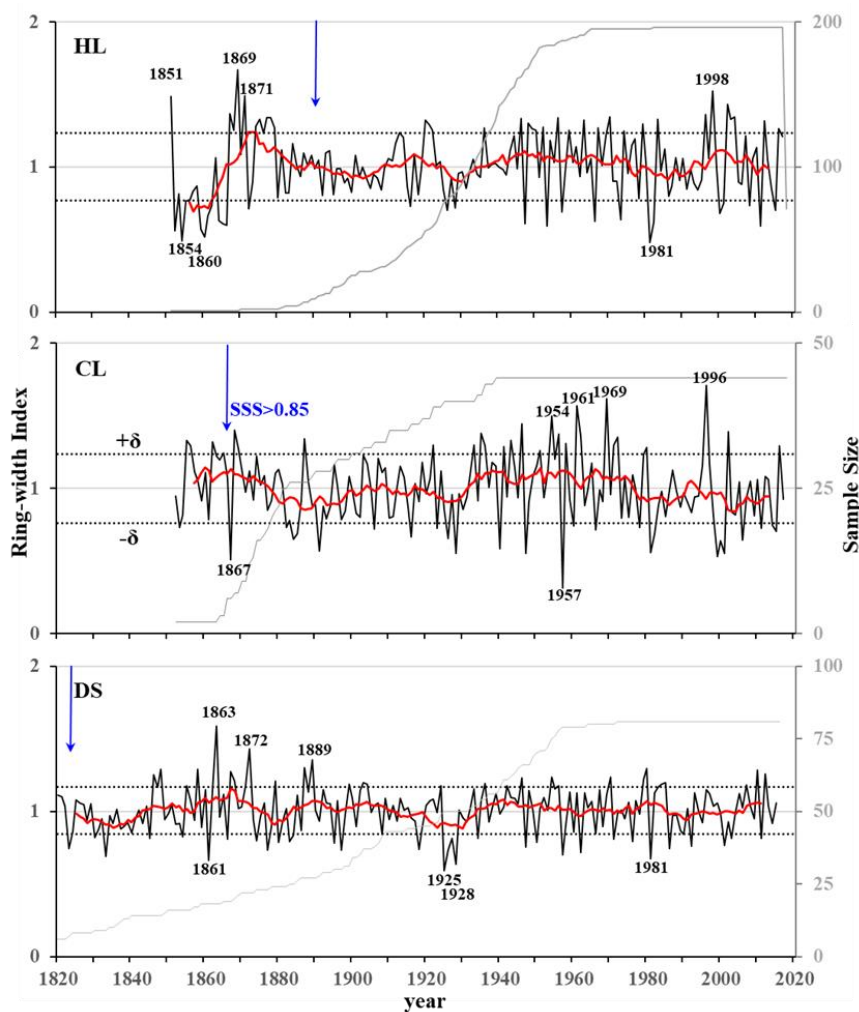
234

235

236 **3. Results and analysis**

237 **3.1 Ring-width chronologies and their characteristics**

238 Based on the sampling cores from five sample sites at HL, two sample sites at DS, and
239 one sample site at CL, ring-width residual chronologies were derived for each of the
240 three study areas (Fig. 3). Statistical parameters showed that the three chronologies
241 meet the usual requirements for correctly done dendrochronological studies. (Table 1).



242

243 Figure 3. Residual ring-width chronologies for the three study areas. The dark lines
 244 indicate the chronology; grey lines indicate the sample depth; red lines indicate the 11-
 245 year running mean chronology; dotted horizontal lines indicate the mean value $\pm 1\delta$,
 246 years with data identified as $>/<$ mean $\pm 2\delta$ (δ : standard deviation); the blue arrows
 247 indicate the start of the reliable residual chronology ($SSS > 0.85$).

248 Table 1. Statistical characteristics of the sampling sites and the tree-ring chronologies.

Sampling sites	HL(5)	CL(1)	DS(2)
Latitude (°N)	38.52–38.97	37.61	39.04
Longitude (°E)	105.83–106.02	103.71	100.78



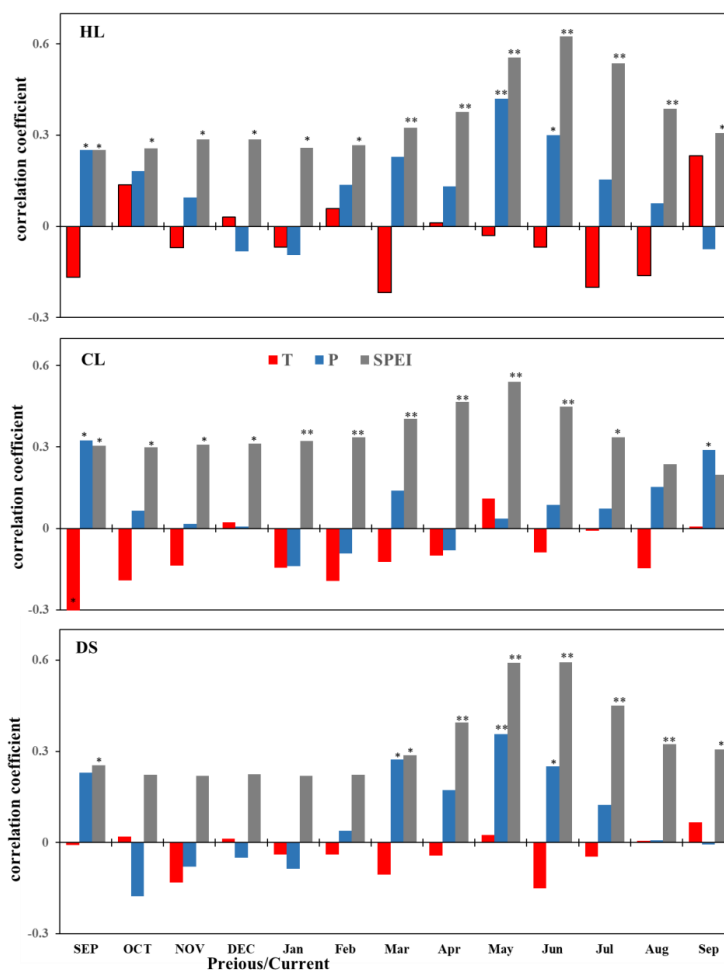
Elevation (m)	2200–2750	2490	2650–2700
Cores	209	48	81
Reliable period	1891–2018	1866–2017	1823–2015
MS	0.18–0.37	0.28	0.15–0.33
Rbar	0.45–0.61	0.56	0.40–0.60
SNR	22.5–56.1	38.9	25.7–42.5
EPS	0.96–0.98	0.98	0.96–0.98
PC1(%)	17.3–63.0	57.9	43.0–62.5

249 Reliable period, MS (mean sensitivity), Rbar (mean series intercorrelation), SNR (signal to noise ratio),
250 EPS (expressed population signal), and PC1 (variance explained by the first principal component) refer
251 to residual chronologies.

252

253 **3.2 Climate response characteristics**

254 Correlation analysis comparing a) monthly mean temperature and precipitation at
255 neighboring meteorological stations and b) SPEI at the nearest grid-point showed that,
256 overall, the three residual chronologies were correlated negatively with monthly mean
257 air temperature, positively correlated with monthly precipitation, and positively
258 correlated with SPEI during the growing season (Fig. 4).



259
 260 Figure 4. Correlation coefficients (Pearson's r values) between the residual ring-width
 261 chronologies of Qinghai spruce at the three study areas (HL, CL and DS) and the
 262 observed monthly temperature (T), total monthly precipitation (P), and SPEI.

263 * Pearson's r correlation, significant at $P < 0.05$.

264 ** Pearson's r correlation, significant at $P < 0.01$.

265 Month names of previous year are capitalized.

266 HL chronology was correlated negatively with mean temperature mainly in C5–C8
 267 in the growing season, but not to the significant level. It was also positively correlated
 268 with precipitation in all months except P12, C1, and C9, reaching significant levels
 269 ($P < 0.05$) in P9, C5, and C6. All months were positively correlated with SPEI and



270 reached statistical significance ($P<0.05$), with C3–C8 showing highly significant
271 correlation levels ($P<0.01$).

272 CL chronology was negatively correlated with mean temperature in all months
273 except for P12, C5 and C9. Only P9 reached statistical significance ($P<0.05$). CL
274 chronology was positively correlated with monthly precipitation, save for C1, C2, and
275 C4. Only P9 and C9 reached statistical significance ($P<0.05$). All months were
276 positively correlated with SPEI, with P9–C7 reaching significant correlation levels
277 ($P<0.05$) and C1–C7 reaching highly significant correlation levels ($P<0.01$).

278 DS chronology showed weak correlations between DS chronology and monthly
279 mean temperatures. None of the correlations reached levels of significance. DS
280 chronology was positively correlated with P9 and C2–C8 precipitation and reached
281 significant correlation levels for C3, C5, and C6 ($P<0.05$). All months were positively
282 correlated with SPEI, with P9 and C3–C9 reaching significant correlation levels
283 ($P<0.05$) and C4–C8 reaching highly significant correlation levels ($P<0.01$).

284 Overall, the radial growth of Qinghai spruce at the three study areas seems to have
285 been limited, for the most part, by low precipitation during the growing season (April–
286 July). The three chronologies reflect regional wet and dry variations.

287

288 3.3 Regional climate changes as recorded by tree-ring widths

289 3.3.1 Regional climate change viewed at interannual scales

290 On interannual scales, the three residual chronologies, when compare, showed highly
291 significant correlations. HL-CL: $n=166$ ($P<0.01$); HL-DS: $n=165$ ($P<0.01$); CL-DS:
292 $n=164$, $P<0.01$). This indicates that there was a high degree of consistency in the radial
293 growth of Qinghai spruce in the three regions.

294 According to the results of the chronology-climate response analysis in the
295 previous section, the high and low ring-width indices ($\text{mean} \pm 1 \sim 2\delta$) of the chronology
296 at the three sample sites indicate wetter or drier, and extreme wet or dry years,
297 respectively (Table 2).

298 Overall, the three ring-width residual chronologies (HL, CL, DS) had a total of two
299 shared wetter years and seven shared drier years. The HL and CL chronologies shared



300 four wet years and eleven dry years; the HL and DS chronologies shared five wet years
 301 and nine dry years; and the CL and DS chronologies shared five wet years and seven
 302 dry years (Table 2).

303 **Table 2. Years of high or low growth, wet or dry climate in the three chronologies**

chronology	Higher index/wetness years ($\geq \text{mean} + 1\delta$)	Lower index/drought years ($\leq \text{mean} - 1\delta$)
HL	1851 , 1867, 1869 , 1871 , 1874, 1875, 1877, 1878, <u>1879</u> , 1920, 1921, <u>1922</u> , <u>1936</u> , <u>1946</u> , 1952, <u>1959</u> , 1963, 1967, <u>1970</u> , 1974, <u>1979</u> , 1983, 1996, 1998 , 2002, 2003, 2004, <u>2012</u> , <u>2016</u>	1852, 1854 , 1855, 1859, 1860 , <u>1861</u> , 1864, 1865, 1866, 1872, <u>1916</u> , <u>1926</u> , <u>1928</u> , <u>1947</u> , 1953, <u>1957</u> , <u>1966</u> , 1973, 1981 , <u>1982</u> , <u>2000</u> , <u>2001</u> , <u>2011</u>
CL	<u>1855</u> , 1862, <u>1922</u> , 1933, 1935, <u>1936</u> , 1941, <u>1946</u> , 1951, 1954 , 1958, 1961 , 1969 , 1972, <u>1980</u> , 1996 , <u>2016</u>	1867 , 1884, 1885, 1891, <u>1916</u> , 1923, <u>1926</u> , <u>1928</u> , <u>1947</u> , 1957 , 1960, <u>1966</u> , 1978, <u>1981</u> , <u>1982</u> , 1999, <u>2000</u> , <u>2001</u> , 2006, <u>2011</u> , 2014, 2015
DS	1846, 1848, <u>1855</u> , 1858, 1863 , 1867, 1868, 1872 , <u>1879</u> , 1887, 1889 , 1899, 1903, 1904, 1924, <u>1936</u> , 1942, <u>1946</u> , <u>1954</u> , 1956, <u>1959</u> , <u>1970</u> , <u>1979</u> , <u>1980</u> , 2007, 2010, <u>2012</u>	1823, 1830, 1833, <u>1854</u> , 1861 , 1874, 1877, 1880, 1883, 1884, 1895, 1897, 1908, 1925 , <u>1926</u> , 1927, 1928 , 1934, <u>1947</u> , 1950, <u>1957</u> , 1962, 1971, 1976, 1981 , 1985, 1990, 1992, <u>2001</u> , 2003, <u>2011</u>

304 Note: Bold is used to indicate **extreme years** ($>/< \text{mean} \pm 2\delta$; δ : standard deviation); double
 305 underlining indicates years shared between two of the three sample sites; bold underlining
 306 shows years shared between three sample sites.

307 There were no extremely wet years shared by the three sample sites. However, there
 308 were two shared wetter years in 1936 and 1946 and several shared wetter years in later
 309 years among the three sample sites. For example, note the wetter years in 1922 and
 310 2016 for HL and DS chronologies; 1959, 1979, and 2012 for HL and DS chronologies;
 311 1855, 1954, and 1980 for CL and DS chronologies (Table 2).

312 The extreme drought years are consistent among the three sample sites. For
 313 instance, there was an extreme drought year in 1981 at HL and DS sample sites; it was
 314 also a drought year at CL. An extreme drought year at CL in 1957 was also a drought
 315 year for the other two chronologies. Moreover, the extreme drought year of 1928 at DS
 316 was a drought year at the other two sites. Drought years in 1926, 1947, 2001, and 2011

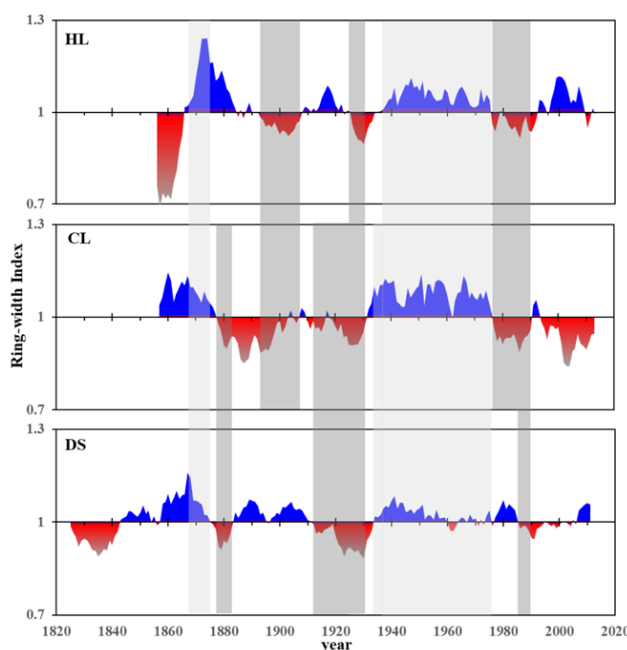


317 were seen in all three sites and in two of the three sample sites (1916, 1966, 1982, and
318 2000 at HL and CL; 1854 and 1861 at HL and DS) (Table 2).

319

320 **3.3.2 Characteristics of regional climate change at inter-decadal scales**

321 On the decadal scale, the 11a running mean series indicates that at the HL site there
322 were four wetter periods (mid-1860s to early 1880s; 1910s to 1920s; mid-1930s to mid-
323 1970s; and late 1990s to early 2010s). Four drought periods were seen (mid-1850s to
324 mid-1860s; early 1890s to late 1900s; circa 1930s; and mid-1970s to 1980s) (Fig.5).



325

326 **Figure 5.** Three regional chronologies demonstrating alternation between dry and wet
327 years on interdecadal scales (11 a running mean). The gray bands indicate consistent
328 changes.

329 The CL regional chronology revealed two main wetter periods (mid-1850s to mid-
330 1870s; mid-1930s to mid-1970s) and two longer drought periods (late 1870s to early
331 1930s; following the late 1970s) (Fig.5).

332 The DS regional chronology showed four main wetter periods (mid-1840s to mid-
333 1870s; mid-1880s to late 1900s; mid-1930s to mid-1980s; and late 2000s to early



334 2010s). There were four drought periods (mid-1820s to mid-1840s; mid-1870s to 1880s;
335 early 1910s to early 1930s; and late 1980s to mid-2000s). The drought during the last
336 drought period was less severe (Fig.5).

337 The three chronologies show both synchronized phases and differential changes on
338 an interdecadal scale. The more synchronized dry phases of climate change were the
339 drought periods of the 1930s and 1990s. When we compared the DS chronology to the
340 HL and CL chronologies on decadal scales, we noted that DS droughts tended to last
341 longer and that they started and ended later than CL droughts. However, HL and DS
342 droughts tended to end at ~~close to~~ the same time (Fig.5).

343 There were two wet periods in 1870s and the mid-1930s to 1970s which were
344 shared by all three sample sites. The latter period was the longest lasting wet period we
345 saw in our study. There were also dry and wet periods that were not shared by any of
346 our sites. There was an HL drought (mid-1850s to mid-1860s) which was not shared by
347 the other two sites, which were wetter. HL and CL shared drought periods (1890s to
348 1910s; 1980s) while DS was wetter. Conversely wetter periods at HL were sometimes
349 accompanied by drought in the other two sites. Drought at CL was sometimes
350 accompanied by wet periods at the other two sites. DS was wet during the 2010s but
351 the other two sites were in drought (Fig.5).

352 The results of the above studies show that there are diversified and complex
353 features in the interdecadal processes of climate change in different regions around the
354 Alxa Plateau.

355

356 **3.4 Driving mechanism of the regional climate changes**

357 **3.4.1 Driving mechanism of the regional climate changes of typical years**

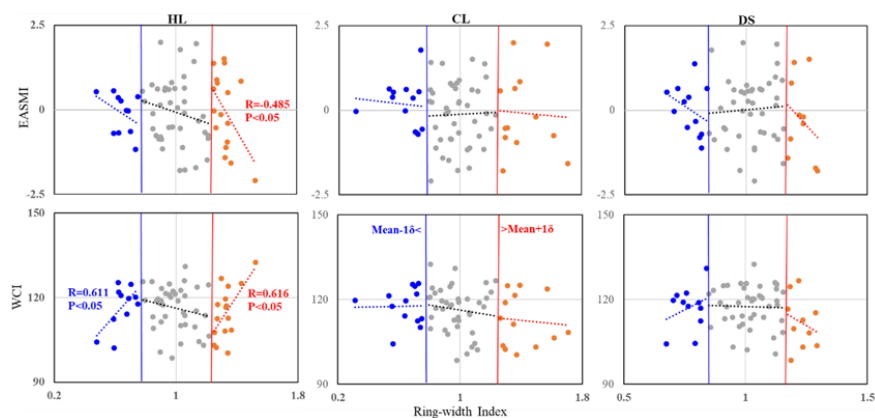
358 On the interannual scales, three regional chronologies we developed showed fairly
359 weak negative correlations between the EASM and the westerlies; none of the
360 correlations were statistically significant. We carried out correlation analyses of the
361 three regional ring-width chronologies and two major circulation indices. This was
362 done in high, medium and low ring-width index groups (Fig. 6; 7).



363 At HL, the results of our combined subgroup correlation analyses suggest that
364 correlations between radial growth groups and atmospheric circulations were stable.
365 Correlation between the higher ring-width group and atmosphere circulation indices
366 and between the lower ring-width group and the WCI were all significant ($P < 0.05$) (Fig.
367 6; 7).

368 At CL, correlations between the higher and middle ring-width groups to the WCI
369 and the higher and middle WCI groups to the ring-width index were all negative.
370 Correlations between the higher and middle ring-width groups and the EASMI, and
371 between the higher and middle EASMI groups with the ring-width index were
372 inconsistent (Fig. 6; 7).

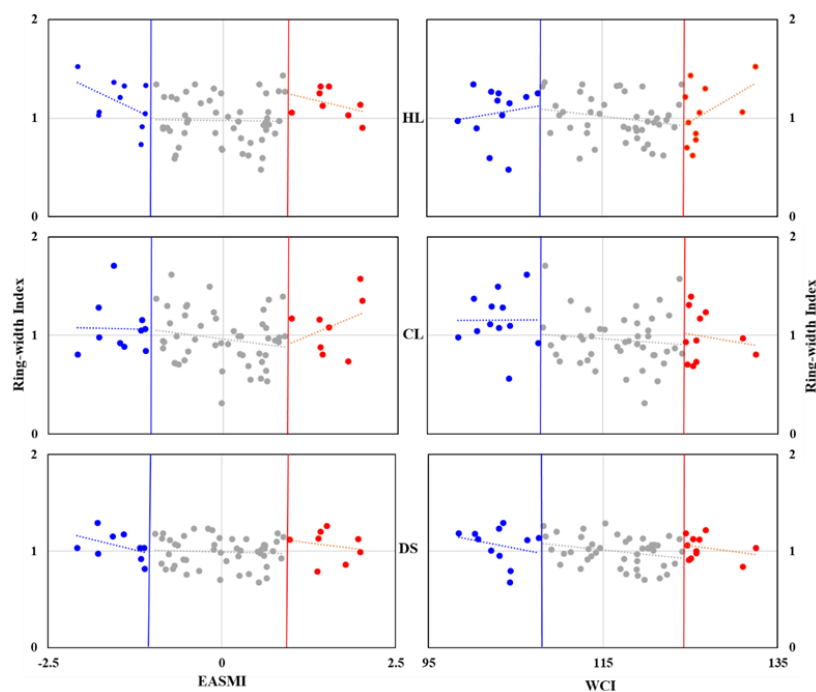
373 At DS, correlations between the higher and lower ring-width groups and the
374 EASMI, and between the higher and lower EASMI groups to the ring-width indices,
375 were consistent. The correlations between the higher ring-width groups and the WCI,
376 and between the higher WCI groups and the ring-width index were consistent. However,
377 the correlations between the lower ring-width groups and the WCI, also between the
378 lower WCI groups and the ring-width index, were inconsistent (Fig. 6; 7).



379
380 **Figure 6.** Grouping related charts among the ring-width index of three regions (HL, CL
381 and DS) and the two atmospheric circulations' indices (EASMI and WCI). The noted
382 numbers are the person correlation coefficients (two-tails test) and the corresponding
383 significant credible level. Red dots indicate the higher ring-width index group



384 (>mean+1δ), gray dots indicate the middle ring-width index group (>mean-1δ~<
385 mean+1δ), and blue dots indicate the lower ring-width index group (>mean-1δ).



386
387 **Figure 7.** Grouping related charts among the two atmosphere circulations' index
388 (EASMI and WCI) and the ring-width index of three regions (HL, CL, and DS). Red
389 dots indicate the higher atmosphere circulations' index group (>mean+1δ), gray dots
390 indicate the middle atmosphere circulations' index group (>mean-1δ~< mean+1δ), and
391 blue dots indicate the lower atmosphere circulations' index group (>mean-1δ).

392 Except for HL, none of the ring-width groups or the atmospheric circulation index
393 groups of the others reached a level of significance. These results suggest that HL is
394 strongly affected by size of, and the interaction between, the EASM and the westerlies.
395 On an interannual scale, stronger west winds and a weaker monsoon could result in
396 variations from the ordinary climate (veering towards drier or wetter). Weaker west
397 winds and a stronger monsoon formed the normal climate at HL. At the CL and DS
398 sites, both atmospheric circulations were relatively weak on interannual scales. They
399 had complex interactions.

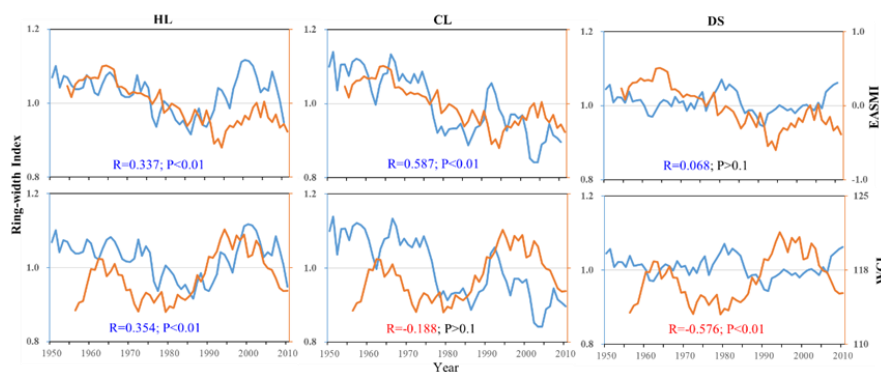
400



401 **3.4.2 Driving mechanisms of the regional climate changes on a decadal scale**

402 At HL, both the EASM and the westerly circulation had highly significant effects on
403 the radial growth of the Qinghai spruce. At CL, the EASM also had highly significant
404 effects on radial growth of the Qinghai spruce. There, correlation coefficients were
405 higher for the EASMI (EASM index) than they were for the HL index. Correlations
406 between the WCI and radial growth were negative, but not at a significant level.

407 At DS, correlation between radial growth and the WCI was extremely negative
408 ($P < 0.01$). Correlation between radial growth and the EASM was positive ($P > 0.1$) (Fig.
409 8). These results suggest that at HL, alternations between dry and wet seasons were
410 affected both by the EASM and the westerlies. If either of the two atmospheric
411 circulations was stronger, the climate tended to be wetter. At CL, alternations between
412 dry and wet were affected mainly by the EASM. When the EASM was stronger, the
413 climate was wetter. At DS, the climate was affected mainly by the westerly winds. The
414 stronger the winds, the wetter the climate (Fig. 8).



415

416 Figure 8. Interdecadal scale (11-a running average) correlations of the three residual
417 chronologies with the EASMI and WCI.

418 The results of our interdecadal partial correlation analysis of the three RES-
419 chronologies with the WCI and EASMI further illustrate the impacts of the two
420 circulation systems on the climate of the three regions (Table 3).

421 At HL, if we control one factor (the WCI or EASMI) from our analysis, the other
422 factor showed a positive correlation ($P < 0.0001$). At CL, if we controlled the WCI, we
423 find a positive significant correlation with EASMI ($P < 0.0001$). If we controlled the



424 effect of EASMI, we saw a weak negative correction with WCI (Table 3). At DS, if we
425 controlled EASMI, we saw a negative significant correlation with WCI ($P < 0.0001$). If
426 we controlled the WCI, we saw an insignificant negative correlation with EASMI
427 (Table 3).

428 Table 3. Inter-decadal partial correlation analysis of the three residual-chronologies
429 with the WCI and EASMI.

	HL	CL	DS
WCI	0.489 ***	0.550***	-0.172
EASMI	0.511***	-0.001	- 0.591***

430 Correlation significance levels (two-tailed test): *** $P < 0.001$.

431 Summary: at HL (on the eastern boundary of the Alxa Plateau), both EASMI and
432 WCI influenced the alternation between wet and dry; at CL (on the southern boundary
433 of the Alxa Plateau), climate was mainly influenced by the EASM. At DS (on the
434 western boundary of the Alxa Plateau and the middle part of Hexi Corridor), climate
435 was mainly influenced by the westerly winds.

436

437 4. Discussion and conclusions

438 4.1 Climate changes indicated by regional chronologies

439 Our chronology-climate response analysis (Fig. 4) showed that the radial growth index
440 of Qinghai spruce in the HL, CL and DS mountains were a good record of regional
441 climate changes around the Alxa Plateau (Fig. 3). On the interannual scale, the three
442 regional chronologies noted that the extreme drought years of 1928, 1957 and 1981
443 were shared by two or more locations, as were the drought years of 1854, 1861, 1916,
444 1926, 1947, 1966, and 2001 (Fig. 3 and Table 3).

445 We note that drought was also reported by other tree-ring studies for these regions
446 (Chen et al., 2016), also for the Qilian Mountains (Zhang et al., 2011; Zhang et al.,
447 2017). Several other drought years (1854, 1884, and 1925–1928) were also seen in the
448 dry-wet climate history (PDSI) (recorded by tree-ring-widths) in the nearby area of



449 Mount Hasi, which lies on the edge of the regions most influenced by the EASM (Kang
450 et al., 2012).

451 The drought years of 1823, 1833, 1854, 1877, 1883–1885, 1895, 1908, 1971, 1992,
452 and 2003 seen in results for the Alxa Plateau are also seen in twelve tree-ring
453 reconstructed drought series for the Qilian Mountains (an area mainly influenced by
454 westerly winds) (Zhang et al., 2011). We also note that wetter years seen in our three
455 regional chronologies were also seen in results from the Hasi and Xinglong Mountains,
456 which are also on the edge of the area influenced by the EASM) (Fang et al., 2009;
457 Kang et al., 2012).

458 If we compare our results with those seen for the EASM-affected areas at Mount
459 Guiqing, 1820–2005 (Fang et al., 2010), we noted that only three of the eight drought
460 years in that area (1928, 2000, and 2001) were seen in our three chronologies. We also
461 noted results from the westerly-influenced area at Mount Tianshan (Jiang et al., 2017).
462 The wetter years of 1846, 1903 and 1942 at DS were also extreme wet years at Mount
463 Tianshan. Two wet years, 1848 and 1959, recorded at DS are either one year earlier or
464 one year later than extremely wet years at Mount Tianshan, which might suggest some
465 correlation. Drier years at DS (1884, 1947 and 1951) are one or two years later than the
466 extremely dry years at Mount Tianshan. This suggests that these phenomena could be
467 related to broader **changes in the extent and strength of the atmospheric circulation.**

468 On a broader (interdecadal) scale, an extreme drought period in 1920s–1930s was
469 shared by much of northern China (Liang et al., 2006; Fang et al., 2009; Fang et al.,
470 2010). This is the same drought that we note our chronologies for HL, CL and DS (Liu
471 et al., 2002; Chen et al., 2010; Fan et al., 2012; Liu et al., 2013; Zhang et al., 2015). A
472 drought in 1890–1900 was noted by dendrochronological studies and regional history
473 documents (Yuan, 1994; Ma et al., 2003; Cai and Liu, 2007).

474 Ma and Fu's (2006) study showed a broad shift towards a drying climate in 1977–
475 78 (eastern area in northwestern China, also northern China). Several other
476 dendrochronological studies showed a combination of high temperatures and low
477 precipitation in the late 1970s to early 1990s (Zhang et al., 2005b; Cai and Liu, 2007;
478 Cai, 2009).



479 This same drought was seen at DS, if somewhat later and for a shorter time. We
480 also noted its effects at HL and CL. This would be consistent with the increased
481 humidity of the climate in the eastern region of Northwest China (the EASM-influenced
482 region experiencing >400 mm precipitation). This region would include Mount
483 Xinglong (Fang et al., 2009; Chen et al. 2015), the easternmost part of the Qilian
484 Mountains, and Mount Guiqing (Fang et al., 2010).

485 The wet period that lasted from the 1940s to the early 1970s has been recorded by
486 several tree-ring-width chronologies covering HL, CL, and DS (Liu et al., 2004; Liu et
487 al., 2005; Gao et al., 2006; Cai, 2009; Chen et al., 2010). Regional history documents
488 also record some severe floods disasters in this period (Yuan, 1994). We also see this
489 wet period in tree-ring-width chronologies from Mount Xinglong (Fang et al., 2009;
490 Chen et al. 2015) and Mount Guiqing (Fang et al., 2010).

491 The wet period in the 1830s–1840s evident in the chronologies in Xinglong
492 Mountain (Fang et al., 2009)(Chen et al. 2015) and Guiqing Mountain (Fang et al., 2010)
493 corresponds to the dry period of DS. The wet period in the 1830s–1840s corresponds
494 to the dry period of HL and CL, and to the wet period of DS. The observed phenomena
495 can be attributed to differences in the extent and intensity of EASM and westerly
496 atmospheric circulations.

497

498 **4.2 Influence of atmospheric circulations and their interaction on climate change** 499 **in the Alxa Plateau**

500 ~~It is known that that~~ water vapor carried by the westerly winds will extend southward
501 to the northern part of Qinghai, the Hexi region of Gansu, the northern part of Ningxia,
502 and the northern part of Shaanxi Province, sometimes passing through the northern
503 border of the Xinjiang region (Li et al., 2012). The area bounded by 35° and 55°N,
504 110°E and 140°E seems to key to fluctuations in the westerly winds. This in turn affects
505 the distribution of rain belts in summer. Its mean WCI are weaker positively to the
506 rainfall in the middle of Yellow River Basin and its northern regions (Yan et al., 2007).
507 The results showed that the middle ring-width index group of Qinghai spruce in the
508 three sample sites, which are located in the key area for interaction between wind and



509 monsoon, presented weaker negative correlation with WCI on the interannual scale (Fig.
510 6).

511 The EASM boundary zone has a greater influence on precipitation at higher
512 latitudes and thus on vegetation growth. This boundary zone can fluctuate due to the
513 interannual variability of the EASM and the westerlies. There may be lagging effects
514 at the mid-latitudes (Ou and Qian, 2006). Again, we note that on an interannual scale,
515 there is much variation in the strengths and interactions of the EASM and westerly
516 circulation and thus on climate in our three study regions (Fig. 6).

517 Sun et al. (2019) showed that when the westerly circulation strengthens, high
518 latitude air pressure drops across the entire Asian continent. Siberian high pressures and
519 the EASM are weakened. The south of the cold air activity is also correspondingly
520 weakened. That is not conducive to the north and south of the cold and warm air vapor
521 exchange to form precipitation. When the lower of the WCI and weakened latitudinal
522 circulation, the meridional circulation will strengthen, which favors the exchange of
523 warm and cold air between the north and south to form precipitation.

524 Yang et al. (2019) proposed that in years with weak summer westerlies in the
525 middle latitudes, the upper-level jet stream tends to shift southward. This southward
526 displacement of the jet stream, coupled with weakened lower-level divergence, hampers
527 the northward transport of warm air into the southwestern region. Consequently, this
528 leads to reduced availability of water vapor sources and ultimately results in diminished
529 summer precipitation within the transitional zone of typical monsoon activity. If the jet
530 stream moves northward, precipitation increases.

531 Xu et al. (2010) wrote that in the middle Qilian Mountains the westerly winds affect
532 precipitation directly, while the EASM only indirectly affects precipitation. When the
533 westerly winds are stronger, the high precipitation zone moves northwestward; when
534 they are weaker, the zone moves.

535 At DS, radial growth showed weak negative correlations with higher WCI and also
536 higher, middle, and lower EASMI groups (Figs. 6;7). At HL, when high chronology
537 indices are positive they are significantly correlated with westerly circulation; when
538 they are negative they significantly correlate with EASM (Figs. 6; 7). At CL, which lies



539 further to the south than HL, a higher EASMI leads to a more humid climate. Other
540 effects are more complicated: for example, the higher and lower ring-width index
541 groups, associated with extreme dry and wet climate years, have weak negative
542 correlations to EASMI (Figs. 6; 7). Jiang et al. (2019) published the results of their
543 hydrogen and oxygen isotope studies of surface water at more than 3,000 sampling sites
544 in northern China. They showed that surface water recharge in the DS Mountains is due
545 to the westerly winds; recharge in the CL Mountains is due to the EASM. The HL
546 Mountains, in contrast, sit at the boundary of the EASM; water recharge there is due to
547 both the EASM and the westerlies.

548 Jiang and Wang (2005) notes significant declines in the EASM in the mid-1960s
549 and mid-1970s, which led to decline in the radial growth of Qinghai spruce in our study
550 area. The effect of the latter declined period was much greater than that of the former,
551 whatever the intensity or duration. The effects of these declines were stronger at CL
552 and DS than at HL. In the mid-1970s, EASM retreat had stronger negative effects at
553 CL and then at HL. However, decline in the EASM proved to be a facilitator of radial
554 growth at DS (Fig. 8).

555 In the same period the westerly circulation also retreated. The EASM retreated
556 again in 1990s, while the westerly winds strengthened. This resulted in a drier climate
557 in the CL Mountains. However, it was also correlated with fluctuating wet periods at
558 HL and a weak wet period at DS. The above results, to a certain extent, support our
559 view on the driving mechanisms of climate change in the three study areas, especially
560 in the DS Mountains.

561 When we look at this area on a geologic scale, we learn that the westerly circulation
562 strengthened during the Ice Age. Westerly jet streams moved southward to about 35°N.
563 When the westerly winds weakened in the Interglacial Age, the westerly jet streams
564 moved northward to ~37°N (Sun et al., 2003). A study of Holocene lake level evolution
565 in the ancient Zhuye lake, central Alxa Plateau, showed that lake-level change was
566 subject to the combined effects of EASM and the arid climate of Central Asia (Li, 2009)
567 This result further illustrates the complexity of lake evolution and climate change in the
568 EASM marginal zone.



569 The westerly circulation also interacts with the monsoon on the Tibetan Plateau,
570 which has a profound effect on the climate of the Asian monsoon region as well as the
571 global climate (Qu et al., 2004). There has also been much research using proxy
572 indicator cycles indicating that our study area is also influenced by large-scale climate
573 and ocean-atmosphere changes on interannual and interdecadal scales, such as the
574 North Atlantic Oscillation (NAO), Pacific Decadal Oscillation (PDO), El Niño-
575 Southern Oscillation (ENSO), and sunspot activity (Gou et al., 2015a; 2015b; Liu et al.,
576 2016; Wang et al., 2017).

577 However, all of the above-mentioned large-scale climate and ocean-atmosphere
578 changes affect the EASM and westerly circulation through different pathways (Li.
579 2009), which in turn have various effects on the northwestern edge zone of the EASM
580 and the zone of interaction between the two major atmospheric circulations.

581 In conclusion, based on the analysis of the regional chronologies collected in the
582 HL, CL and DS mountains that are arrayed around the Alxa Plateau, we can safely assert
583 that the radial growth of Qinghai spruce in the study area is mainly affected by regional
584 precipitation. This precipitation varies constantly over time and space, primarily
585 influenced by the interactions between two atmospheric circulation systems, EASM
586 and westerly winds. At HL, both of these atmospheric circulation systems play a
587 significant role in shaping climate changes. At CL, the climate is mainly influenced by
588 the EASM. At DS, climate is more heavily influenced by the westerly circulation.

589 In the future, it is to be hoped that more refined, smaller scale research can be done
590 on the climate history in the deserts of the Alxa Plateau. Such research may finally to
591 provide a theoretical basis to explain regional climate driving mechanisms and thus
592 enable better desertification controls.

593

594 **Competing interests:** The contact author has declared that none of the authors has any
595 competing interests.

596

597 **Acknowledgements**



598 The study was jointly funded by the National Natural Science Foundation of China
599 (NSFC) (No.42171031; 42171167); Inner Mongolia Autonomous Region Special Fund
600 project for transformation of Scientific and technological Achievements (2021CG0046).

601

602 **References**

603 Cai, Q. F.: Response of *Pinus tabulaeformis* tree-ring growth to three moisture indices and
604 January to July Walter index reconstruction in Helan mountain, Marine geology &
605 Quaternary geology, 29, 131–136 (In Chinese with English abstract),
606 <https://doi.org/10.3724/SP.J.1140.2009.06131>, 2009.

607 Cai, Q. F. and Liu, Y.: January to August temperature variability since 1776 inferred from tree-
608 ring width of *Pinus tabulaeformis* in Helan Mountain, Journal of Geographical Sciences,
609 17, 293–303, <https://doi.org/10.1007/s11442-007-0293-5>, 2007.

610 Chen, F., Yuan, Y. J., Zhang, T. W., and Linderholm, H. W.: Annual precipitation variation for
611 the southern edge of the Gobi Desert (China) inferred from tree rings: linkages to climatic
612 warming of twentieth century, Nat. Hazards, 81, 939–955, <https://doi.org/10.1007/s11069-015-2113-z>, 2016.

614 Chen, F., Wei, W. S., Yuan, Y. J., Yu, S. L., Shang, H. M., Zhang, T. W., Zhang, R. B., Wang, H.
615 Q., and Qin, L.: Variation of annual precipitation during 1768–2006 in Gansu Inferred from
616 multi-site tree-ring chronologies, Journal of Desert Research, 33, 1520–1526 (In Chinese
617 with English abstract), <https://doi.org/10.7522/j.issn.1000-694X.2013.00218.>, 2013.

618 Chen, F., Yuan, Y. J., Wei, W. S., Yu, S. L., Fan, Z. A., Zhang, R. B., Zhang, T. W., Li, Q., and
619 Shang, H. M.: Temperature reconstruction from tree-ring maximum latewood density of
620 Qinghai spruce in middle Hexi Corridor, China, Theoretical and Applied Climatology, 107,
621 633–643, <https://doi.org/10.1007/s00704-011-0512-y>, 2012.

622 Chen, F., Yuan, Y. J., Wei, W. S., Yu, S. L., Li, Y., Zhang, R., Fan, Z., Zhang, T., and Shang, H.:
623 PDSI changes of May to July recorded by tree rings in the northern Helan Mountains,
624 Advance in Climate Changes Research, 65, 344–348 (In Chinese with English abstract),
625 2010.

626 Chen, F. H., Chen, J. H., Huang, W., Chen, S. Q., Huang, X. Z., Jin, L. Y., Jia, J., Zhang, X. J.,
627 An, C., and Zhang, J.: Westerlies Asia and monsoonal Asia: spatiotemporal differences in
628 climate change and possible mechanisms on decadal to sub-orbital timescales, Earth-Sci.
629 Rev., 192, 337–354, <https://doi.org/10.1016/j.earscirev.2019.03.005>, 2019a.

630 Chen, F. H., Fu, B. J., Xia, J., Wu, D., Wu, S. H., Zhang, Y. L., Sun, H., Liu, Y., Fang, X. M.,
631 Qin, B. Q., Li, X., Zhang, T. J., Liu, B. Y., Dong, Z. B., Hou, S. G., Tian, L. D., Xu, B. Q.,
632 Dong, G. H., Zheng, J. Y., Yang, W., Wang, X., Li, Z. J., Wang, F., Hu, Z. B., Wang, J.,
633 Liu, J. B., Chen, J. H., Huang, W., Hou, J. Z., Cai, Q. F., Long, H., Jiang, M., Hu, Y. X.,
634 Feng, X. M., Mo, X. G., Yang, X. Y., Zhang, D. J., Wang, X. H., Yin, Y. H., and Liu, X.
635 C.: Major advances in studies of the physical geography and living environment of China



- 636 during the past 70 years and future prospects, *Science China Earth Sciences*, 62, 1665–
637 1701, <https://doi.org/10.1007/s11430-019-9522-7>, 2019b.
- 638 Chen, J., Huang, W., Jin, L., Chen, J. H., Chen, S. Q., and Chen, F. H.: A climatological northern
639 boundary index for the East Asian summer monsoon and its interannual variability,
640 *Science China Earth Sciences*, 61, 13–22, <https://doi.org/10.1007/s11430-017-9122-x>,
641 2018.
- 642 Ding, Y. H., Liu, Y. J., Xu, Y., Wu, P., Xue, T., Wang, J., Shi, Y., Zhang, Y. X., Song, Y. F., and
643 Wang, P. L.: Regional responses to global climate change: progress and prospects for trend,
644 causes, and projection of climatic warming-wetting in Northwest China, *Advances in
645 Earth Science*, 38, 551–562 (In Chinese with English abstract),
646 <https://doi.org/10.11867/j.issn.1001-8166.2023.027>, 2023.
- 647 Fan, Z. A., Wei, W. S., Chen, F., and Yuan, Y. J.: Precipitation variation from 1775 to 2005 at
648 the eastern margin of Tengger Desert, China inferred from tree-ring, *Journal of Desert
649 Research*, 32, 996–1002 (In Chinese with English abstract), 2012.
- 650 Fang, K. Y., Gou, X. H., Chen, F. H., D'arrigo, R., and Li, J. B.: Tree-ring based drought
651 reconstruction for the Guiqing Mountain (China): linkages to the Indian and Pacific
652 Oceans, *Int. J. Climatol.*, 30, 1137–1145, <https://doi.org/10.1002/joc.1974>, 2010.
- 653 Fang, K. Y., Gou, X. H., Chen, F. H., Yang, M. X., Li, J. B., He, M. S., Zhang, Y., Tian, Q. H.,
654 and Peng, J. F.: Drought variations in the eastern part of northwest China over the past two
655 centuries: evidence from tree rings, *Clim. Res.*, 38, 129–135,
656 <https://doi.org/10.3354/cr00781>, 2009.
- 657 Feng, W., Wang, K. L., and Jiang, H.: Influences of westerly wind inter-annual change on water
658 vapor transport over northwest china summer, *Plateau Meteorology*, 23, 270–275 (In
659 Chinese with English abstract), 2004.
- 660 Gao, S. Y., Lu, R. J., Qiang, M. R., Ha, S., Zhang, D. S., Chen, Y., and Xia, H.: Precipitation
661 variation recorded by tree-rings in the northern Tengger Desert of the last 140 years, *Chin.
662 Sci. Bull.*, 51, 326–331, <https://doi.org/10.1360/csb2006-51-3-326>, 2006.
- 663 Gou, X. H., Gao, L. L., Deng, Y., Chen, F. H., Yang, M. X., and Still, C.: An 850 - year tree -
664 ring - based reconstruction of drought history in the western Qilian Mountains of
665 northwestern China, *Int. J. Climatol.*, 35, 3308–3319, <https://doi.org/10.1002/joc.4208>,
666 2015a.
- 667 Gou, X. H., Deng, Y., Gao, L. L., Chen, F. H., Cook, E., Yang, M. M., and Zhang, F.: Millennium
668 tree-ring reconstruction of drought variability in the eastern Qilian Mountains, northwest
669 China, *Climate Dynamics*, 45, 1761–1770, <https://doi.org/10.1007/s00382-014-2431-y>,
670 2015b.
- 671 Huang, L. X., Chen, J., Yang, K., Yang, Y. J., Huang, W., Zhang, X., and Chen, F. H.: The
672 northern boundary of the Asian summer monsoon and division of westerlies and monsoon
673 regimes over the Tibetan Plateau in present-day, *Science China Earth Sciences*, 66, 882–
674 893, <https://doi.org/10.1007/s11430-022-1086-1>, 2023.



- 675 Jiang, D. B. and Wang, H. J.: Natural interdecadal weakening of East Asian summer monsoon
676 in the late 20th century, *Chin. Sci. Bull.*, 50, 1923–1929, [https://doi.org/10.1360/982005-](https://doi.org/10.1360/982005-36)
677 36, 2005.
- 678 Jiang, P., Liu, H. Y., Wu, X. C., and Wang, H. Y.: Tree-ring-based SPEI reconstruction in central
679 Tianshan Mountains of China since A.D. 1820 and links to westerly circulation, *Int. J.*
680 *Climatol.*, 37, 2863–2872, <https://doi.org/10.1002/joc.4884>, 2017.
- 681 Jiang, W. J., Wang, G. C., Sheng, Y. Z., Shi, Z. M., and Zhang, H.: Isotopes in groundwater (^2H ,
682 ^{18}O , ^{14}C) revealed the climate and groundwater recharge in the Northern China, *Sci. Total*
683 *Environ.*, 666, 298–307, <https://doi.org/10.1016/j.scitotenv.2019.02.245>, 2019.
- 684 Kang, S. Y. and Yang, B.: Precipitation variability at the northern fringe of the Asian summer
685 monsoon in Northern China and its possible mechanism over the past 530 years,
686 *Quaternary Sciences*, 35, 1185–1193, [https://doi.org/10.11928/j.issn.1001-](https://doi.org/10.11928/j.issn.1001-7410.2015.05.14)
687 7410.2015.05.14, 2015.
- 688 Kang, S. Y., Yang, B., and Qin, C.: Recent tree-growth reduction in north central China as a
689 combined result of a weakened monsoon and atmospheric oscillations, *Clim. Change*, 115,
690 519–536, <https://doi.org/10.1007/s10584-012-0440-6>, 2012.
- 691 Li, D. L., Shao, P. C., and Wang, H.: The position variations of the north boundary of East Asia
692 subtropical summer monsoon in 1951–2009, *Journal of Desert Research*, 33, 1511–1519
693 (In Chinese with English abstract), <https://doi.org/10.7522/j.issn.1000-694X.2013.00217>,
694 2013.
- 695 Li, J. L., Li, Z. R., Yang, J. C., Shi, Y. Z., and Fu, J.: Analyses on spatial distribution and
696 temporal variation of atmosphere water vapor over northwest China in summer of later 10
697 years, *Plateau Meteorology*, 31, 1574–1581 (In Chinese with English abstract), 2012.
- 698 Li, J. P. and Zeng, Q. C.: A new monsoon index, its interannual variability and related with
699 monsoon precipitation, *Climatic and Environmental Research*, 10, 351–365 (In Chinese
700 with English abstract), 2005.
- 701 Li, W. L., Wang, K. L., Fu, S. M., and Jiang, H.: The interrelationship between regional Westerly
702 index and the water vapor budget in Northwest China, *Journal of Glaciology and*
703 *Geocryology*, 30, 28–34 (In Chinese with English abstract), 2008.
- 704 Li, Y.: The pollen records from lake sediments and climate & lake model in the Marginal area
705 of Asian monsoon, Lanzhou University, Lanzhou, China, 2009.
- 706 Li, Z. X., Feng, Q., Song, Y., Wang, Q. J., Yang, J., Li, Y. G., Li, J. G., and Guo, X. Y.: Stable
707 isotope composition of precipitation in the south and north slopes of Wushaoling Mountain,
708 northwestern China, *Atmospheric Research*, 182, 87–101,
709 <https://doi.org/10.1016/j.atmosres.2016.07.023>, 2016.
- 710 Liang, E. Y., Liu, X. H., Yuan, Y. J., Qin, N. S., Fang, X. Q., Huang, L., Zhu, H. F., Wang, L.,
711 and Shao, X. M.: The 1920s drought recorded by tree rings and historical documents in
712 the semi-arid and arid areas of Northern China, *Clim. Change*, 79, 403–432,
713 <https://doi.org/10.1007/s10584-006-9082-x>, 2006.



- 714 Liu, J. B., Chen, J., Chen, S. Q., Yan, X. W., Dong, H. R., and Chen, F. H.: Dust storms in
715 northern China and their significance for the concept of the Anthropocene, *Science China*
716 *Earth Sciences*, 65, 921–933, <https://doi.org/10.1007/s11430-021-9889-8>, 2022.
- 717 Liu, Y., Cai, Q. F., Ma, L. M., and An, Z. S.: Tree ring precipitation records from Baotou and
718 the East Asia summer monsoon variations for the last 254 years, *Earth Sci. Front.*, 8, 91–
719 97 (In Chinese with English abstract), <https://doi.org/10.3321/j.issn:1005-2321.2001.01.012>, 2001.
- 721 Liu, Y., Sun, C. F., Li, Q., and Cai, Q. F.: A *Picea crassifolia* tree-ring width-based temperature
722 reconstruction for the Mt. Dongda region, Northwest China, and its relationship to large-
723 scale climate forcing, *PLoS One*, 11, e0160963,
724 <https://doi.org/10.1371/journal.pone.0160963>, 2016.
- 725 Liu, Y., Lei, Y., Sun, B., Song, H. M., and Li, Q.: Annual precipitation variability inferred from
726 tree-ring width chronologies in the Changling–Shoulu region, China, during AD 1853–
727 2007, *Dendrochronologia*, 31, 290–296, <https://doi.org/10.1016/j.dendro.2013.02.001>,
728 2013.
- 729 Liu, Y., Won-Kyu, P., Cai, Q. F., Jung-Wook, S., and Hyun-Sook, J.: Monsoonal precipitation
730 variation in the East Asia since A.D. 1840—tree-ring evidences from China and Korea,
731 *Science in China Series D: Earth Sciences*, 46, 1031–1039,
732 <https://doi.org/10.1007/BF02959398>, 2003.
- 733 Liu, Y., Ma, L. M., Cai, Q. F., An, Z. S., Liu, W. G., and Gao, L. Y.: Reconstruction of summer
734 temperature (June–August) at Mt. Helan, China, from tree-ring stable carbon isotope
735 values since AD 1890, *Science in China Series D: Earth Sciences*, 45, 1127–1136,
736 <https://doi.org/10.1360/02yd9109>, 2002.
- 737 Liu, Y., Cai, Q. F., Liu, W. G., Yang, Y. K., Sun, J. Y., Song, H. M., and Li, X. X.: Monsoon
738 precipitation variation recorded by tree-ring $\delta^{18}\text{O}$ in arid Northwest China since AD 1878,
739 *Chemical Geology*, 252, 56–61, <https://doi.org/10.1016/j.chemgeo.2008.01.024>, 2008.
- 740 Liu, Y., Cai, Q. F., Shi, J. F., Hughes, M. K., Kutzbach, J. E., Liu, Z. Y., Ni, F. B., and An, Z. S.:
741 Seasonal precipitation in the south-central Helan Mountain region, China, reconstructed
742 from tree-ring width for the past 224 years, *Canadian Journal of Forest Research*, 35,
743 2403–2412, <https://doi.org/10.1139/x05-168>, 2005.
- 744 Liu, Y., Shi, J. F., Shishov, V., Vaganov, E., Yang, Y. K., Cai, Q. F., Sun, J. Y., Wang, L., and
745 Djanseitov, I.: Reconstruction of May–July precipitation in the north Helan Mountain,
746 Inner Mongolia since A.D. 1726 from tree-ring late-wood widths, *Chin. Sci. Bull.*, 49,
747 405–409, <https://doi.org/10.1007/BF02900325>, 2004.
- 748 Ma, L. M., Liu, Y., Cai, Q. F., and An, Z. S.: The precipitation records from tree-ring late wood
749 width in the helan mountain, *Marine geology & Quaternary geology*, 23, 109–114 (In
750 Chinese with English abstract), <https://doi.org/10.16562/j.cnki.0256-1492.2003.04.016>,
751 2003.
- 752 Ma, M. J., Pu, Z. X., Wang, S. G., and Zhang, Q. A.: Characteristics and numerical simulations



- 753 of extremely large atmospheric boundary-layer heights over an arid region in north-west
754 china, *Boundary-Layer Meteorology*, 140, 163–176, [https://doi.org/10.1007/s10546-011-](https://doi.org/10.1007/s10546-011-9608-2)
755 9608-2, 2011.
- 756 Ma, Z. G. and Fu, C. B.: The basic facts of aridity in northern China from 1951 to 2004, *Chin.*
757 *Sci. Bull.*, 51, 2429–2439 (In Chinese), <https://doi.org/10.1360/csb2006-51-20-2429>,
758 2006.
- 759 Ou, T. H. and Qian, W. H.: Vegetation variations along the monsoon boundary zone in East
760 Asia, *Chinese Journal of Geophysics*, 49, 698–705 (In Chinese with English abstract),
761 2006.
- 762 Qin, L., Liu, G. X., Li, X. Z., Chongyi, E., Li, J., Wu, C. R., Guan, X., and Wang, Y.: A 1000-
763 year hydroclimate record from the Asian summer monsoon-Westerlies transition zone in
764 the northeastern Qinghai-Tibetan Plateau, *Clim. Change*, 176, 1–20,
765 <https://doi.org/10.1007/s10584-023-03497-1>, 2023.
- 766 Qu, W. J., Zhang, X. H., Wang, D., Shen, Z. X., Mei, F. M., Cheng, Y., and Yan, L. W.: The
767 important significance of westerly wind study, *Marine Geology and Quaternary Geology*,
768 24, 125–132 (In Chinese with English abstract), [https://doi.org/10.16562/j.cnki.0256-](https://doi.org/10.16562/j.cnki.0256-1492.2004.01.018)
769 1492.2004.01.018, 2004.
- 770 Shao, X. M., Xu, Y., Yin, Z. Y., Liang, E. Y., Zhu, H. F., and Wang, S.: Climatic implications of
771 a 3585-year tree-ring width chronology from the northeastern Qinghai-Tibetan Plateau,
772 *Quaternary Science Reviews*, 29, 2111–2122,
773 <https://doi.org/10.1016/j.quascirev.2010.05.005>, 2010.
- 774 Sun, D. H., An, Z. S., Su, R. H., Deer, H. Y., and Sun, Y. B.: The dust deposition records of the
775 evaluation of Asia monsoon and Westerly circulation in north China in the last 2.6Ma,
776 *Science in China (Series D)*, 33, 497–504 (In Chinese), 2003.
- 777 Sun, L. Q., Li, T. J., Li, Q. L., and Wu, Y. P.: Responses of autumn flood peak in the Yellow
778 River source regions to westerly circulation index, *Journal of Glaciology and Geocryology*,
779 41, 1475–1482 (In Chinese with English abstract), [https://doi.org/10.7522/j.issn.1000-](https://doi.org/10.7522/j.issn.1000-0240.2019.0028)
780 0240.2019.0028, 2019.
- 781 Tang, X., Qian, W. H., and Liang, P.: Climatic features of boundary belt for East Asian Summer
782 Monsoon, *Plateau Meteorology*, 25, 375–381 (In Chinese with English abstract), 2006.
- 783 Wang, B. J., Huang, Y. X., He, J. H., and Wang, L. J.: Relation between vapour transportation
784 in the period of East Asian Summer Monsoon and drought in Northwest China., *Plateau*
785 *Meteorology*, 23, 912–917 (In Chinese with English abstract), 2004.
- 786 Wang, J. L., Yang, B., Ljungqvist, F. C., Luterbacher, J., Osborn, Timothy j., Briffa, K. R., and
787 Zorita, E.: Internal and external forcing of multidecadal Atlantic climate variability over
788 the past 1,200 years, *Nature Geoscience*, 10, 512–517, <https://doi.org/10.1038/ngeo2962>,
789 2017.
- 790 Wang, K. L., Jiang, H., and Zhao, H. Y.: Atmospheric water vapor transport from westerly and
791 monsoon over the Northwest China, *Advances in Water Science*, 16, 432–438 (In Chinese



- 792 with English abstract), <https://doi.org/10.14042/j.cnki.32.1309.2005.03.021>, 2005.
- 793 Xiao, S. C., Chen, X. H., and Ding, A. J.: Study process of climate changes, environment
794 evolution and its driving mechanism in the last two centuries in the Alxa Desert, *Journal*
795 *of Desert Research*, 37, 1102–1201 (In Chinese with English abstract),
796 [10.7522/j.issn.1000-694x.2017.00002](https://doi.org/10.7522/j.issn.1000-694x.2017.00002), 2017.
- 797 Xiao, S. C., Yan, C. Z., Tian, Y. Z., Si, J. H., Ding, A. J., Chen, X. H., Han, C., and Teng, Z. Y.:
798 Regionalization for desertification control and countermeasures in the Alxa Plateau, China,
799 *Journal of Desert Research*, 39, 182–192 (In Chinese with English abstract),
800 <https://doi.org/10.7522/j.issn.1000-694X.2019.00068>, 2019.
- 801 Xu, J. J., Wang, K. L., Jiang, H., Li, Z. G., Sun, J., Luo, X. P., and Zhu, Q. L.: A numerical
802 simulation of the effects of Westerly and Monsoon on precipitation in the Heihe River
803 Basin, *Journal of Glaciology and Geocryology*, 32, 489–496 (In Chinese with English
804 abstract), 2010.
- 805 Yan, H. S., Hu, J., Fan, K., and Zhang, Y. J.: The analysis of relationship between the variations
806 of Westerly Index in summer and precipitation during the flood period over China in the
807 last 50 years. , *Chinese Journal of Atmospheric Science*, 31, 717–726 (In Chinese with
808 English abstract), 2007.
- 809 Yang, B., Qin, C., Wang, J. L., He, M. H., Melvin, T. M., Osborn, T. J., and Briffa, K. R.: A
810 3,500-year tree-ring record of annual precipitation on the northeastern Tibetan Plateau,
811 *Proc. Natl. Acad. Sci. USA*, 111, 2903–2908, <https://doi.org/10.1073/pnas.1319238111>,
812 2014.
- 813 Yang, J. H., Zhang, Q., Liu, X. Y., Yue, P., Shang, J. L., Ling, H., and Li, W. J.: Spatial-temporal
814 characteristics and causes of summer precipitation anomalies in the transitional zone of
815 typical summer monsoon, China, *Chinese Journal of Geophysics*, 62, 4120–4128 (In
816 Chinese with English abstract), <https://doi.org/10.6038/cjg2019M0639>, 2019.
- 817 Yuan, L.: *Hazards history in northwestern China*, Gansu people's press, Lanzhou, China 1994.
- 818 Zhang, F., Chen, Q. M., Su, J. J., Deng, Y., Gao, L. L., and Gou, X. H.: Tree-ring recorded of
819 the drought variability in the northwest monsoon marginal, China, *Journal of Glaciology*
820 *and Geocryology*, 39, 245–251 (In Chinese with English abstract),
821 <https://doi.org/10.7522/j.issn.1000-0240.2017.0028>, 2017.
- 822 Zhang, Q., Yang, J. H., Wang, P. L., Yu, H. P., Yue, P., Liu, X. Y., Lin, J. J., Duan, X. Y., Zhu,
823 B., and Yan, X. Y.: Progress and prospect on climate warming and humidification in
824 Northwest China, *Chin. Sci. Bull.*, 68, 1814–1828, <https://doi.org/10.1360/TB-2022-0643>,
825 2023.
- 826 Zhang, Q. B., Cheng, G. D., Yao, T. D., Kang, X. C., and Huang, J. G.: A 2,326 year tree-ring
827 record of climate variability on the northeastern Qinghai-Tibetan Plateau, *Geophys. Res.*
828 *Lett.*, 30, 1739, <https://doi.org/10.1029/2003GL017425>, 2003.
- 829 Zhang, Q. L., Liu, W. G., Liu, Y., Ning, Y. F., and Wen, Q. B.: Relationship between the stable
830 carbon and oxygen isotopic compositions of tree ring in the Mt. Helan region,



- 831 Northwestern China, *Geochimica*, 34, 51–56, [https://doi.org/10.19700/j.0379-](https://doi.org/10.19700/j.0379-1726.2005.01.006)
832 1726.2005.01.006, 2005a.
- 833 Zhang, S., Xu, H., Lan, J. H., Goldsmith, Y., Torfstein, A., Zhang, G. L., Zhang, J., Song, Y. P.,
834 Zhou, K. E., Tan, L. C., Xu, S., Xu, X. M., and Enzel, Y.: Dust storms in northern China
835 during the last 500 years, *Science China Earth Sciences*, 64, 813–824,
836 <https://doi.org/10.1007/s11430-020-9730-2>, 2021.
- 837 Zhang, Y., Shao, X. M., Yin, Z. Y., Liang, E. Y., Tian, Q. H., and Xu, Y.: Characteristics of
838 extreme droughts inferred from tree-ring data in the Qilian Mountains, 1700–2005, *Clim.*
839 *Res.*, 50, 141–159, <https://doi.org/10.3354/cr01051>, 2011.
- 840 Zhang, Y. X., Yu, L., and Yin, H.: Annual precipitation reconstruction over last 191 years at the
841 south edge of Badain Jaran Desert based on tree ring width data, *Desert and Oasis*
842 *Meteorology*, 9, 12–16 (In Chinese with English abstract),
843 <https://doi.org/10.3969/j.issn.1002-0799.2015.01.003>, 2015.
- 844 Zhang, Y. X., Gou, X. H., Hu, W. D., Peng, J. F., and Liu, P. X.: The drought events recorded
845 in tree ring width in Helan Mt. over past 100 years, *Acta Ecologica Sinica*, 25, 2121–2126
846 (In Chinese with English abstract), 2005b.
847